Enhancing endogenous adenosine A_{2A} receptor signaling induces slow-wave sleep without affecting body temperature and cardiovascular function

Mustafa Korkutata[a, b], Tsuyoshi Saitoh[a], Yoan Cherasse[a], Shuji Ioka[a], Feng Duo[c], Rujie Qin[c], Nobuyuki Murakoshi[c], Shinya Fujii[a], Xuzhao Zhou[a], Fumihiro Sugiyama[d], Jiang-Fan Chen[e], Hidetoshi Kumagai[f], Hiroshi Nagase[a], and Michael Lazarus[a, *]

[a]International Institute for Integrative Sleep Medicine (WPI-IIIS), University of Tsukuba, Tsukuba, Ibaraki 305-8575, Japan

[b]Ph.D. Program in Human Biology, School of Integrative and Global Majors, University of Tsukuba, Tsukuba, Ibaraki 305-8577, Japan

[c]Cardiovascular Division, Faculty of Medicine, Graduate School of Comprehensive Human Sciences, University of Tsukuba, Tsukuba, Ibaraki 305-8575, Japan

[d]Laboratory of Animal Resource Center, Faculty of Medicine, University of Tsukuba, Tsukuba, Ibaraki 305-8575, Japan

[e]Department of Neurology, Boston University School of Medicine, Boston, MA 02118, USA

[f]Department of Cardiovascular Medicine, Graduate School of Medicine, The University of Tokyo, Bunkyo-ku, Tokyo 113-8654, Japan

*Corresponding Author: Dr. Michael Lazarus, Principal Investigator and Associate Professor, International Institute for Integrative Sleep Medicine, University of Tsukuba, 1-1-1 Tennodai, Tsukuba, Ibaraki 305-8575, Japan, Phone/fax: 81-29-853-3681, Email: lazarus.michael.ka@u.tsukuba.ac.jp

Abstract

Insomnia is one of the most common sleep problems with an estimated prevalence of 10% to 15% in the general population. Although adenosine A_{2A} receptor ($A_{2A}R$) agonists strongly induce sleep, their cardiovascular effects preclude their use in treating sleep disorders. Enhancing endogenous $A_{2A}R$ signaling, however, may be an alternative strategy for treating insomnia, because adenosine levels in the brain accumulate during wakefulness. In the present study, we found that 3,4-difluoro-2-((2-fluoro-4-iodophenyl)amino)benzoic acid, denoted $A_{2A}R$ positive allosteric modulator (PAM)-1, enhanced adenosine signaling at the $A_{2A}R$ and induced slow wave sleep (SWS) without affecting body temperature in wild-type male mice after intraperitoneal administration, whereas the SWS-inducing effect of this benzoic acid derivative was abolished in $A_{2A}R$ KO mice. In contrast to the $A_{2A}R$ agonist CGS 21680, the $A_{2A}R$ PAM-1 did not affect blood pressure or heart rate. These findings indicate that enhancing $A_{2A}R$ signaling promotes SWS without cardiovascular effects. Therefore, small molecules that allosterically modulate $A_{2A}Rs$ could help people with insomnia to fall asleep.

Keywords

Adenosine A_{2A} receptor, allosteric modulator, insomnia, slow-wave-sleep, body temperature, cardiovascular function

Abbreviations

CHO, Chinese hamster ovary; EEG, electroencephalography; EMG, electromyography; ECG, electrocardiography; PAM, positive allosteric modulator; REM, rapid eye movement; SWS, slow-wave sleep.

1. Introduction

Insomnia is one of the most common sleep problems with an estimated prevalence of 10% to 15% in the general population and 30% to 60% in the older population (Roth, 2007). Moreover, insomnia frequently co-occurs with a wide range of psychiatric disorders, including depression and anorexia (de Zambotti et al., 2017; Seow et al., 2018). The most widely prescribed agents for the treatment of insomnia are benzodiazepines and non-benzodiazepines, which are central nervous system depressants that enhance signaling of the inhibitory neurotransmitter γ-aminobutyric acid (Wafford and Ebert, 2008). These medications, however, are plagued by a wide range of adverse effects, including muscle relaxation, rebound insomnia, changes in appetite, next-day sedation, cognitive impairment, amnesic effects, and development of drug tolerance and dependence (Aragona, 2000; Vgontzas et al., 1995). Orexin receptor antagonists were also recently developed and approved for treating insomnia (Cox et al., 2010). The major issues of these drugs are next-morning sleepiness with possible muscle weakness, strange dreams, sleep-walking, and other nighttime behaviors or suicidal ideation (Jacobson et al., 2014). Moreover, because orexin receptor antagonists mostly work by preventing arousal from sleep, they are generally ineffectual in people who have problems falling asleep. A highly selective adenosine A_{2A} receptor ($A_{2A}R$) agonist, CGS 21680, produces profound increases in sleep after infusion into the subarachnoid space underlying the ventral surface region of the rostral basal forebrain in rats, the lateral ventricle of mice, or the lateral preoptic area of rats (Satoh et al., 1999; Scammell et al., 2001; Urade et al., 2003; Methippara et al., 2005). Administration of an $A_{2A}R$ agonist is not considered to have clinical potential for the treatment of sleep disorders, however, due to its adverse cardiovascular effects, which include hypotension and tachycardia (de Lera Ruiz et al., 2014). A positive allosteric

modulator (PAM) may evoke selective physiologic $A_{2A}R$ responses because, in contrast to an $A_{2A}R$ agonist, its actions are limited to when and where adenosine is released. Adenosine levels in the brain progressively increase during wakefulness (Porkka-Heiskanen et al., 1997), and therefore allosteric modulation of $A_{2A}Rs$ to promote the somnogenic effects of the increased adenosine may be an alternative strategy for treating insomnia.

In the present study, we identified a small lipophilic monocarboxylate (3,4-difluoro-2-((2-fluoro-4-iodophenyl)amino)benzoic acid), denoted $A_{2A}R$ PAM-1, that induces slow-wave sleep (SWS), the major part of sleep characterized by slow and high-voltage brain waves, by enhancing $A_{2A}R$ signaling without affecting body temperature, blood pressure, or heart function in mice.

2. Material and methods

2.1. Reagents

Adenosine (Nacalai Tesque, Kyoto, Japan), CGS 21680 (Sigma-Aldrich, St. Louis, MO), Cremophor® EL (Sigma-Aldrich), DMSO (Nacalai Tesque), DMEM (Nacalai Tesque), FBS (Nichirei Biosciences, Tokyo, Japan), HBSS (Gibco, Waltham, MA), hygromycin B (Wako, Tokyo, Japan), ketamine hydrochloride (Ketalar, Daiichi Sankyo, Tokyo, Japan), nonessential amino acids (NEAA; Nacalai Tesque), penicillin/streptomycin (Wako), pentobarbital (Somnopentyl, Kyoritsu Seiyaku, Tokyo, Japan), puromycin (InvivoGen, San Diego, CA), saline (Otsuka, Tokyo, Japan), Ultrance cAMP-kit (PerkinElmer, Waltham, MA), xylazine hydrochloride (Celactal, Bayer, Tokyo, Japan), ZM241385 (Tocris Bioscience, Bristol, UK), 3-isobutyl-1-methylxanthine (IBMX; Tocris Bioscience) and HEPES (Gibco).

106 *2.2. Animals*

107 Male mouse lines on a C57BL/6 background, including wild-type and $A_{2A}R$ KO (Chen
108 et al., 1999) mice, which were maintained at the International Institute of Integrative
109 Sleep Medicine and weighing 21-27 g (10-15 weeks old), were used in the experiments.
110 The animals were housed in an insulated and soundproof recording chamber that was
111 maintained at an ambient temperature of 23 ± 0.5°C with a relative humidity of 50 ±
112 5% and an automatically controlled 12 h light/12 h dark cycle (light on at 8:00,
113 illumination intensity ≈ 100 lux). All animals had free access to food and water. This
114 study was performed in strict accordance with the recommendations in the Guide for
115 the Care and Use of Laboratory Animals of the US National Institutes of Health (2011).
116 Experimental protocols were in compliance with relevant Japanese and institutional
117 laws and guidelines and approved by the University of Tsukuba animal ethics
118 committee (protocol #14-322). Every effort was made to minimize the number of
119 animals used as well as any pain and discomfort experienced by the animals.
120

121 *2.3. Mouse $A_{2A}R$-expressing Chinese hamster ovary cells*

122 The flag epitope-tagged open reading frame of $A_{2A}R$ was amplified by PCR from
123 mouse brain total RNA. The resultant amplicon was cloned into a pMXs-IRES-Puro
124 retroviral vector (Kitamura et al., 2003). The plasmid was then transfected into the
125 retrovirus packaging cell line Plat-E (Morita et al., 2000). The supernatant of
126 transfected Plat-E cells was recovered after 24 h and applied to Chinese hamster ovary
127 (CHO) cells strongly expressing the ecotropic receptor for the retrovirus (Montminy et
128 al., 1990). Mouse $A_{2A}R$-expressing CHO ($mA_{2A}R$-CHO) cells were selected in DMEM
129 supplemented with 5% FBS and 1% NEAA by treatment with hygromycin B (250
130 $\mu g \cdot ml^{-1}$) and puromycin (10 $\mu g \cdot ml^{-1}$). The $mA_{2A}R$-CHO cells were subsequently

maintained in DMEM supplemented with 5% FBS, 1% NEAA, 1% penicillin/streptomycin, and 250 $\mu g \cdot ml^{-1}$ hygromycin B at 37°C in an atmosphere of 5% CO_2.

2.4. cAMP assay

Activation of A_{2A}Rs was quantified by cyclic adenosine monophosphate (cAMP) accumulation in CHO cells expressing mouse A_{2A}Rs. CHO cells were suspended in HBSS containing 1 M HEPES and 0.25 M IBMX in 384-well micro-plates (2×10^3 cells/well), and incubated with adenosine and A_{2A}R PAM-1 at the indicated concentrations for 30 min at 25°C. The detection mixture containing the Eu-cAMP tracer and ULight-anti-cAMP antibody was added and incubated for 1 h at 25°C. A micro-plate reader (ARVO X5, Perkin Elmer; excitation: 340 nm; emission: 665 nm) was used to measure the Förster resonance energy transfer (FRET) signal. All experiments were performed according to the manufacturer's instructions (LANCE Ultra cAMP Kit, PerkinElmer). The cAMP levels are based on the dynamic range ("linear portion") of the cAMP standard curve and normalized to the baseline or adenosine treated group.

2.5. Stereotaxic surgery for the placement of EEG/EMG electrodes

Mice were anesthetized with pentobarbital [50 $mg \cdot kg^{-1}$, intraperitoneal (i.p.)] and then placed in a stereotaxic apparatus. Electroencephalogram (EEG) and electromyogram (EMG) electrodes for polysomnographic recordings were chronically implanted in the mice (Oishi et al., 2016). The implant comprised two stainless steel screws (1 mm in diameter) inserted through the skull above the cortex (anteroposterior, +1.0 mm; left-right, -1.5 mm from bregma or lambda) according to the atlas of Paxinos and Franklin

(Paxinos and Franklin, 2004) that served as the EEG electrodes. Two insulated, stainless steel Teflon-coated wires were placed bilaterally into both trapezius muscles and served as the EMG electrodes. All electrodes were attached to a micro connector and fixed to the skull with dental cement.

2.6. Pharmacologic treatment and infusion cannula implantation

For control data, mice were injected with saline or vehicle (10 ml·kg^{-1} body weight, i.p.) at 22:00 or 21:30, respectively. A_{2A}R PAM-1 was dissolved in saline immediately before use and administered intraperitoneally at 22:00 on the experimental day at a dose of 30, 60, or 75 mg·kg^{-1}. ZM241385 (15 mg·kg^{-1}, i.p.) was dissolved in vehicle (5% DMSO, 5% Cremophor® EL in saline) and injected into C57BL/6J mice at 21:30. Mice were randomly assigned to groups that received control or drug injections.

For intracerebroventricular (i.c.v.) infusion of A_{2A}R PAM-1, a stainless-steel cannula was inserted into mice during surgery 0.5 mm anterior and 1.6 mm lateral to bregma to a depth of 1.6 mm below the dura at an angle of 20°, thus placing the cannula into the lateral ventricle. To ensure correct placement of cannula, a plastic tube filled with saline was attached to the infusion cannula; a drop in the meniscus indicated that the cannula tip was in the ventricle. During the experiments, the mice were infused continuously using an infusion pump with artificial cerebrospinal fluid into the lateral ventricle of the brain at a speed of 1 µl·h^{-1}. Sleep-wakefulness states were monitored for a period of 36 h after infusion of each compound. Saline infusion recordings were obtained in each animal for 36 h, beginning at 20:00, which served as the control for the same animal. In the next experiment, A_{2A}R PAM-1 (200 nmol·h^{-1}) was infused into the lateral ventricle of the mouse brain for 12 h (20:00 to 8:00).

2.7. Vigilance state assessment based on EEG/EMG polygraphic recordings

Ten days after surgery, the mice were individually housed in transparent barrels in an insulated soundproof recording chamber and connected to the EEG-EMG recording cables for 3 to 5 days of habituation before starting the polygraphic recordings. To evaluate the spontaneous sleep-wake cycle, each animal was recorded for 24 h beginning at 20:00, the onset of the dark period. The animals then entered the pharmacologic phase of the study in which sleep-wakefulness parameters were recorded for 36 h. The data collected during the first 24 h also served as baseline comparison data for the second experimental day. Cortical EEG/EMG recordings were amplified, filtered (EEG 0.5-30 Hz; EMG 20-200 Hz), and digitized at a sampling rate of 128 Hz, and then recording using data acquisition software SleepSign® (Kissei Comtec, Matsumoto, Japan). The vigilance states were classified offline in 10-s epochs into three stages, i.e., wakefulness, rapid eye movement (REM) sleep, and SWS by SleepSign® (ver 3.4) according to standard criteria (Oishi et al., 2016). As a final step, defined vigilance stages were examined visually, and corrected when necessary.

2.8. Blood pressure and heart rate measurement

The blood pressure of the mice was measured using the tail-cuff method with a BP-98A blood pressure device (Softron, Tokyo, Japan). The same time period (13:00 – 16:00) was selected for testing the blood pressure of each mouse (9-12 weeks old) to avoid normal daily variations in blood pressure. Five consecutive days were used to habituate the mice to the device. To optimize cardiovascular circulation, mice were wrapped in a cotton sheet and, except for the tail, maintained at 37°C within a cylinder heater. A programmable sensor with an inflatable balloon attached to a tail cuff was used to monitor tail pulse waves and measure blood pressure when the pulse waves

were stable and rhythmic. Blood pressure measurement was read and recorded by the software. After five consecutive training days, mice were randomly assigned to one of three groups and injected with saline (10 ml·kg^{-1}, i.p.), A_{2A}R PAM-1 (75 mg·kg^{-1}, i.p.) or CGS 21680 (1 mg·kg^{-1}, i.p.). Blood pressure was measured at 30 min, 1 h 30 min, and 2 h 30 min after injection (at each time-point, 20 readings for each mouse were collected). After testing, the mice were gently picked up by the tail and gently returned to their cages.

The heart rate of the mice was measured by telemetry. Mice were anesthetized with ketamine hydrochloride (80 mg·kg^{-1}, i.p.) and xylazine hydrochloride (8 mg·kg^{-1}, i.p.) and a PhysioTel F20-ETA mouse telemetry transmitter (Data Science International, St. Paul, MN) was placed in the midline of the mouse back and fixed with surgical sutures. The negative (white) electrode was placed in the trapezius muscle, while the positive (red) electrode was sutured to a muscle in the back opposite the xiphoid process. Each mouse was singly housed in a cage after surgery with a distance of at least 1 m between cages to avoid interference between telemetry transmitters. After 7 days of recovery, the mice were randomly assigned to one of three groups and injected with saline (10 ml·kg^{-1}, i.p.), A_{2A}R PAM-1 (75 mg·kg^{-1}, i.p.), or CGS 21680 (1 mg·kg^{-1}, i.p.). The transmitted cardiovascular signal was analyzed for 2 h after the injections using Data Science International software.

2.9. Heart rhythm measurement

The cardiac rhythm of mice was measured by electrocardiography (ECG). Mice were anesthetized with ketamine hydrochloride (80 mg·kg^{-1}, i.p.) and xylazine hydrochloride (8 mg·kg^{-1}, i.p.) and fixed with needles on a styrofoam platform. Mice were then gently pushed into a position where the two front paws and the left rear paw are in contact

with 25-gauge needles that served as ECG electrodes. For intracardiac electrography, the throat of the mice was opened and the internal jugular vein was isolated to insert a catheter along the course of the vein to the right atrium. Electrographic signals were 5.000-10.000-fold amplified and filtered (0.5-250 Hz) with an AC-601G system (Nihon Kohden, Tokyo, Japan). The same time period (10:00 – 12:00) was selected for testing the heart rhythm to avoid normal daily variations in the cardiac rhythm. Mice were randomly assigned to groups that received $A_{2A}R$ PAM-1 (75 $mg \cdot kg^{-1}$, i.p.) or CGS 21680 (1 $mg \cdot kg^{-1}$, i.p.) injections. After recording the baseline for 1-2 minutes, mice were injected with drugs and recording continued for 30 minutes. The data were analyzed using LabChart Pro software (ADInstruments, Dunedin, New Zealand).

2.10. Body temperature measurement

The core body temperature of the mice was measured using Thermochron iButtons (KN Laboratories, Osaka, Japan). iButtons were programmed to monitor core body temperature every 5 min for 14 consecutive days beginning at the end of the recovery period. The mice were anesthetized with pentobarbital (50 mg·kg-1, i.p.). The skin of the abdomen was shaved and cleaned with 70% ethanol and a longitudinal, 2-cm incision was made along the midline. One iButton cleaned with 70% ethanol was placed in the peritoneal cavity and the incision was closed with nylon sutures. The mice were housed individually in cages after surgery and experiments were conducted after a 10-day recovery period. iButtons were removed from the animals after cervical dislocation under anesthesia and RhManager software (KN Laboratories, Osaka, Japan) was used to collect the recorded data from the iButtons.

2.11. Synthesis of $A_{2A}R$ PAM-1

A solution of 2,3,4-fluorobenzoic acid (1.35 g, 7.68 mmol), 2-fluoro-4-iodoaniline (1.91 g, 8.06 mmol), and lithium amide (0.702 g, 30.6 mmol) in tetrahydrofuran (10.5 mL) was reacted using a standard method (Cai et al., 2008) to give 3,4-difluoro-2-((2-fluoro-4-iodophenyl)amino)benzoic acid (A_{2A}R PAM-1, 2.99 g, 99%) as a brown solid (**Figure S1)**; IR (KBr) 3311, 1673, 1602, 1520, 1500, 1444, 1273, 768 cm^{-1}; ^{1}H NMR (400 MHz CD_3OD) δ = 7.89 (1 H, ddd, *J* = 2.3, 6.0, 9.2 Hz), 7.48 (1 H, dd, *J* = 1.8, 10.5 Hz), 7.41 (1 H, ddd, *J* =1.4, 1.8, 8.5 Hz), 6.91 (1 H, ddd, *J* = 7.3, 9.4, 9.4 Hz), 6.75 (1 H, ddd, *J* = 5.6, 8.5, 8.5 Hz); ^{13}C NMR (100 MHz acetone-d_6) δ = 169.9, 155.7 (dd, $J_{C,F}$ = 252.1, 4.8 Hz), 155.6 (d, $J_{C,F}$ = 252.1 Hz), 143.6 (dd, $J_{C,F}$ = 247.8, 14.9 Hz), 137.4 (dd, $J_{C,F}$ = 7.7, 2.9 Hz), 135.0 (d, $J_{C,F}$ = 3.8 Hz), 131.9(d, $J_{C,F}$ = 11.5 Hz), 129.8 (dd, $J_{C,F}$ = 9.6, 3.8 Hz), 125.8 (d, $J_{C,F}$ = 21.0 Hz), 123.8 (d, $J_{C,F}$ = 5.8 Hz), 116.4, 110.1 (d, $J_{C,F}$ = 18.2 Hz), 84.7 (d, $J_{C,F}$ = 6.7 Hz); HRMS-ESI: *m/z* $[M-H]^-$ calcd for C13H6F3INO2, 391.9395; measured, 391.9414.

2.12. Formation of the sodium salt of A_{2A}R PAM-1

Aqueous sodium hydroxide (100 μM, 754 μL) was added to a stirred solution of A_{2A}R PAM-1 (0.266 g, 75.4 mmol) in ethanol (20.0 mL) at 0°C. The mixture was stirred for 45 min at room temperature and then concentrated in vacuo and freeze-dried. The residue was dissolved in water and filtered. The filtrate was freeze-dried to obtain the sodium salt of A_{2A}R PAM-1 (0.265 g, 89%) as a gray solid (m.p. 290−291°C; Anal. Calcd for $C_{13}H_6NO_2 \cdot Na \cdot 1.5H_2O$: C, 35.32; H, 2.05; N, 3.17. Measured: C, 35.34; H, 1.91; N, 3.14). The sodium salt of A_{2A}R PAM-1 was used for all *in-vivo* experiments.

2.13. Statistical analysis

Statistical analyses were carried out using Systat Software (SigmaPlot). All results are presented as mean ± standard error of the mean (SEM). Two-tailed Student's *t*-tests were used for statistical comparisons between two groups (Fig. 1A, B, D, E, Fig. 2C, D, F, Fig. 3B, D, Fig. 4B, Fig. 5A, B, Fig. S2A, B, Fig. S4B, Fig. S5A-C, and Fig. S6A-C). For *t*-tests, the normality of each dataset was established using the Kolmogorov–Smirnov test. Two-way repeated-measures analysis of variance (ANOVA) followed by the Tukey test were used for dose-response effects on the amounts of the SWS, REM sleep, and wakefulness (Fig. 2B, Fig. 3A, C, Fig. 4A, Fig. S3A and Fig. S5A) (Chrivia et al., 1993). In all of the cases, $P < 0.05$ was considered significant (significance levels are indicated in figures as *: $P<0.05$, **: $P<0.01$ or ***: $P<0.001$).

3. Results

3.1. Screening of small-molecule compounds for allosteric $A_{2A}R$ modulation

We established CHO cells that express mouse A_{2A}Rs (**Figure S2**) using a retrovirus-mediated gene transfer method (Kitamura et al., 2003). We used these mA_{2A}R-CHO cells to screen 1173 small-molecule compounds for their allosteric effects at A_{2A}Rs. The compounds were synthesized in Dr. Hiroshi Nagase's laboratory at the University of Tsukuba. A_{2A}R activity in CHO cells was determined by measuring cAMP produced after adding adenosine and small-molecule compounds using a fluorescence resonance energy transfer immunoassay. Because a one-compound-one-well approach may be wasteful research conduct due to a likely small number of active compounds in our library, we tested initially 391 mixtures containing three compounds each in triplicates. We selected mixtures that significantly enhanced the effects of adenosine at the A_{2A}Rs ($P<0.01$, unpaired *t*-test) for individual compound testing and found that eight of the mixtures showed an effect according to this criterion (Mixture 124: $t_{(4)}=27.9$, $P<0.0001$,

Mixture 181: $t_{(4)}$=31.5, P<0.0001, Mixture 194: $t_{(4)}$=30.9, P<0.0001, Mixture 211: $t_{(4)}$=9.6, P=0.0006, Mixture 274: $t_{(4)}$=11, P=0.0003, Mixture 319: $t_{(4)}$=6.81, P=0.0024, Mixture 332: $t_{(4)}$=8.62, P=0.0009, Mixture 346: $t_{(4)}$=4.71 P=0.0091, unpaired t-test; **Figure 1A**). Further individual testing of compounds in the eight mixtures revealed that only compound 371 (3,4-difluoro-2-((2-fluoro-4-iodophenyl)amino)benzoic acid) in mixture 124 enhanced adenosine-induced A_{2A}R activation ($t_{(4)}$=9.14, P=0.0007, unpaired t-test; **Figure 1B**). A cell culture bioassay revealed that cAMP levels were not altered by treating A_{2A}R-expressing or native CHO cells with compound 371 in the absence of adenosine or by treating native CHO with adenosine and compound 371 (**Figure 1C**), suggesting that compound 371 is likely a positive allosteric modulator for A_{2A}Rs, and we therefore named this compound A_{2A}R PAM-1. Co-treatment of A_{2A}R-expressing CHO cells with 150 nM adenosine and various concentrations of A_{2A}R PAM-1 (i.e., 25, 50, and 100 μM) amplified adenosine A_{2A}R-evoked cAMP accumulation in a dose-dependent manner by 42% ± 1.4%, 46% ± 1.1%, and 50% ± 1.0%, respectively (25 μM A_{2A}R PAM-1: $t_{(4)}$=4.47, P=0.011, 50 μM A_{2A}R PAM-1: $t_{(4)}$=7.21, P=0.0019, 50 μM A_{2A}R PAM-1 vs. 25 μM A_{2A}R PAM-1: $t_{(4)}$=4.71, P=0.0092, 100 μM A_{2A}R PAM-1: $t_{(4)}$=9 P=0.0008, 100 μM A_{2A}R PAM-1 vs. 25 μM A_{2A}R PAM-1: $t_{(4)}$=8.08, P=0.0012, 100 μM A_{2A}R PAM-1 vs. 50 μM A_{2A}R PAM-1: $t_{(4)}$=3.65, P=0.021, unpaired t-test; **Figure 1D**). Similarly, co-treatment of A_{2A}R-expressing CHO cells with 100 μM A_{2A}R PAM-1 and 50, 100, or 150 nM adenosine increased A_{2A}R activity in the CHO cells in a dose-dependent manner by 55% ± 0.4%, 66% ± 1.5%, and 72% ± 1.7%, whereas 100 μM A_{2A}R PAM-1 did not significantly enhance the cellular activity of A_{2A}R-expressing CHO cells treated with 250 nM adenosine (50 nM Adenosine: $t_{(4)}$=14.9, P=0.0001, 50 nM Adenosine vs. 100 nM Adenosine: $t_{(4)}$=7.04, P=0.0021, 50 nM Adenosine vs. 150 nM Adenosine: $t_{(3)}$=12.40, P=0.0011, 50 nM

Adenosine vs. 250 nM Adenosine: $t_{(4)}$=11.79, P=0.00029, 100 nM Adenosine: $t_{(4)}$=6.18, P=0.034, 150 nM Adenosine: $t_{(3)}$=4.98, P=0.015, unpaired t-test; **Figure 1E**).

3.2. Intraperitoneal administration of A_{2A}R PAM-1 induces SWS without affecting body temperature in mice

We then tested the effect of intraperitoneal administration of A_{2A}R PAM-1 on the sleep/wake behavior of wild-type mice. We analyzed EEG and EMG recordings made after saline or A_{2A}R PAM-1 injections during the dark period at 22:00, when mice usually spend most of their time awake. Although baseline sleep and wake of mice 24 h prior to treatment was not significantly different between the saline and A_{2A}R PAM-1 groups during the dark period (**Figure S3**), A_{2A}R PAM-1 dose-dependently increased SWS after the injections for the following 8 h (SWS: $F_{(1,106)}$=13.97, P=0.033, two way repeated measures ANOVA-Tukey test, 30 mg·kg^{-1} A_{2A}R PAM-1 vs. 60 mg·kg^{-1} A_{2A}R PAM-1: $t_{(7)}$=4.36, P=0.0032, 30 mg·kg^{-1} A_{2A}R PAM-1 vs. 75 mg·kg^{-1} A_{2A}R PAM-1: $t_{(6)}$=5.45, P=0.0015, unpaired t-test; **Figure 2A, B, D**). The total amount of SWS was increased by 60.8 ± 11.4 min for 8 h with the highest dose of A_{2A}R PAM-1 (i.e., 75 mg·kg^{-1}) compared with saline treatment, whereas wakefulness was decreased by 59.2 ± 12.8 min (SWS: $t_{(7)}$=4.27, P=0.0036, Wake: $t_{(7)}$=4.33, P=0.0034, unpaired t-test; **Figure 2C**). Intraperitoneal injection of A_{2A}R PAM-1 did not significantly alter the REM sleep duration during the dark period compared with saline injection.

Administration of A_{2A}R PAM-1 (75 mg·kg^{-1}, i.p.) to the mice did not significantly affect the episode numbers of SWS and REM sleep for 8 h in the dark period (**Figure S4A**). On the other hand, wake episode numbers lasting 120 to 239 s increased by 307% ($t_{(7)}$=3.88, P=0.006, unpaired t-test), and wake episode numbers lasting 480 to 959 s and 960 to 1909 s decreased by 47% ($t_{(7)}$=2.89, P=0.02, unpaired t-test) and 88%

($t_{(7)}$=4.60, P=0.002, unpaired t-test), respectively, compared with the saline injection. The mean duration of wake episodes decreased by 38% ($t_{(7)}$=3.38, P=0.01, unpaired t-test) compared with saline, but the duration of the SWS and REM sleep episodes was not significantly different after $A_{2A}R$ PAM-1 (75 mg·kg^{-1}, i.p.) administration (**Figure S4B**). $A_{2A}R$ PAM-1 (75 mg·kg^{-1}, i.p.) also did not significantly affect the number of transitions between SWS, wake, and REM sleep (**Figure S4C**).

To assess whether EEG activity was altered by $A_{2A}R$ PAM-1 administration, we compared the normalized EEG power spectrum of SWS in mice treated with saline or $A_{2A}R$ PAM-1 (**Figure 2E**). EEG activity in the frequency range of 0.5–25 Hz during SWS was indistinguishable between $A_{2A}R$ PAM-1–induced and natural (saline injection) SWS. These data suggest that $A_{2A}R$ PAM-1 induced physiologic sleep rather than abnormal sleep.

We also measured the effect of intraperitoneal administration of 75 mg·kg^{-1} $A_{2A}R$ PAM-1 or 1 mg·kg^{-1} of the $A_{2A}R$ agonist CGS 21680 (as positive control) on the body temperature of the mice during the dark period (**Figure 2F**). Although CGS 21680 strongly decreased the body temperature for almost 2 h ($t_{(10)}$=3.68, P=0.0042 at 22:15, $t_{(10)}$=10.48, P<0.0001 at 23:15, $t_{(10)}$=2.33, P=0.041 at 00:05 vs. saline injected group, unpaired t-test), $A_{2A}R$ PAM-1 did not affect the body temperature of the mice. These data suggest that $A_{2A}R$ PAM-1 induces physiologic sleep independent of the body temperature.

3.3. Sleep-inducing effect of $A_{2A}R$ PAM-1 was suppressed by blocking $A_{2A}Rs$

We further investigated whether $A_{2A}Rs$ mediate the sleep-inducing effect of $A_{2A}R$ PAM-1. First, we pretreated wild-type mice with the selective $A_{2A}R$ antagonist ZM241385 (15 mg·kg^{-1}, i.p.) or vehicle 30 min before the $A_{2A}R$ PAM-1 injection at

22:00. The dose of ZM241385 was selected based on previous studies (El Yacoubi et al., 2000; Nakamura et al., 2016). In the presence of ZM241385, A_{2A}R PAM-1 injection produced no significant changes in SWS (**Figure 3A**), indicating that ZM241385 completely blocked the A_{2A}R PAM-1–induced SWS. When we calculated the total amount of SWS for 4 h after the intraperitoneal injection of A_{2A}R PAM-1 (**Figure 3B**), we found that it did not significantly alter the total amount of SWS after ZM241385 pretreatment. ZM241385 pretreatment alone also had no significant effect on SWS compared with vehicle pretreatment (Vehicle + Saline vs. Vehicle + 75 mg·kg^{-1} A_{2A}R PAM-1: $t_{(8)}$=4.04, P=0.0037, 15 mg·kg^{-1} ZM241385 + 75 mg·kg^{-1} A_{2A}R PAM-1 vs. Vehicle + 75 mg·kg^{-1} A_{2A}R PAM-1: $t_{(8)}$=2.63, P=0.029, 15 mg·kg^{-1} ZM241385 + Saline vs. Vehicle + 75 mg·kg^{-1} A_{2A}R PAM-1: $t_{(8)}$=6.10, P=0.00028, unpaired t-test; **Figure 3B**).

We then administered 75 mg·kg^{-1} A_{2A}R PAM-1 (i.p.) into A_{2A}R KO mice and their wild-type littermates at 22:00. We observed no significant changes in SWS in the A_{2A}R KO mice compared with saline treatment, whereas SWS was increased by 74.3 ± 12.0 min for 6 h in wild-type littermates of A_{2A}R KO mice ($F_{(1,190)}$=20.83, P=0.003, two way repeated measures ANOVA-Tukey test, $t_{(14)}$=5.63, P<0.0001, unpaired t-test; **Figure 3C, D**). Concomitantly, wakefulness was decreased in the wild-type littermates of A_{2A}R KO mice ($F_{(1,190)}$=16.14, P=0.005, two way repeated measures ANOVA-Tukey test, $t_{(14)}$=5.50, P<0.0001, unpaired t-test), whereas neither REM sleep in these mice nor wakefulness and REM sleep in the KO mice were affected by intraperitoneal administration of 75 mg·kg^{-1} A_{2A}R PAM-1 (**Figure S5**). Baseline sleep and wake of the KO mice and their wild-type littermates 24 h prior to treatment was not different between the saline and A_{2A}R PAM-1 groups during the dark period (data not shown). These findings suggest that A_{2A}R are necessary for A_{2A}R PAM-1 to induce SWS.

405

406 *3.4. Intracerebroventricular administration of A_{2A}R PAM-1 induces SWS in mice*

407 To elucidate whether the sleep-inducing effect of A_{2A}R PAM-1 is mediated via A_{2A}Rs
408 expressed in the brain, we infused A_{2A}R PAM-1 into the lateral ventricle of wild-type
409 mice at 200 nmol·h^{-1} during the dark period (20:00 to 8:00) and assessed EEG and
410 EMG activity. Infusion with A_{2A}R PAM-1 for 12 h increased the time spent in SWS 5
411 h after the infusion, resulting in a total SWS increase during the dark period of 141.6 ±
412 12.5 min compared with saline infusion ($F_{(1,118)}$=34.40, P=0.004, two way repeated
413 measures ANOVA-Tukey test, $t_{(8)}$=5.67, P=0.00047, unpaired t-test; **Figure 4A, B)**.
414 Concomitantly, total wakefulness was decreased by 145.5 ± 15.8 min during a 12-h
415 i.c.v. infusion of A_{2A}R PAM-1 ($F_{(1,118)}$=43.46, P=0.003, two way repeated measures
416 ANOVA-Tukey test, $t_{(8)}$=5.08, P=0.00095, unpaired t-test), whereas REM sleep was
417 not affected.

418 Intracerebroventricular infusion of A_{2A}R PAM-1 (200 nmol·h^{-1}) into mice affected
419 SWS and wake episode numbers during the dark period (**Figure S6A**). SWS episode
420 numbers lasting 0 to 29 s, 30 to 59 s, and 60 to 120 s increased by 267% ($t_{(8)}$=7.56,
421 P<0.0001, unpaired t-test), 196% ($t_{(8)}$=3.47, P=0.008, unpaired t-test), and 154%
422 ($t_{(8)}$=2.88, P=0.02, unpaired t-test), respectively, and wake episode numbers lasting 0
423 to 29 s, 30 to 59 s, and 60 to 120 s also increased by 205% ($t_{(8)}$=3.97, P =0.004, unpaired
424 t-test), 177% ($t_{(8)}$=3.55, P=0.007, unpaired t-test), and 137% ($t_{(8)}$=2.77, P=0.02,
425 unpaired t-test), respectively, compared with saline infusion. On the other hand, episode
426 numbers of REM sleep were not significantly affected by A_{2A}R PAM-1 infusion (200
427 nmol·h^{-1}, i.c.v.). The mean duration of wake episodes decreased by 72% ($t_{(8)}$=3.06,
428 P=0.01, unpaired t-test) compared with the saline-infused group, but mean episode
429 duration of the SWS and REM sleep did not significantly change after A_{2A}R PAM-1

(200 nmol·h^{-1}, i.c.v.) administration (**Figure S6B**). A_{2A}R PAM-1 (200 nmol·h^{-1}, i.c.v.) increased the number of transitions between SWS and wakefulness by 148% ($t_{(8)}$=4.91, P =0.001, unpaired t-test), and from wakefulness to SWS by 128% ($t_{(8)}$=4.26, P=0.002, unpaired t-test) compared with the saline-infused group (**Figure S6C**).

Moreover, the EEG activity in the frequency range of 0.5–25 Hz during SWS episodes was indistinguishable between mice treated with saline or A_{2A}R PAM-1 (**Figure 4C**). These data suggest that A_{2A}R PAM-1 induces physiologic sleep rather than abnormal sleep via A_{2A}Rs that are likely expressed in the brain.

3.5. Intraperitoneal administration of A_{2A}R PAM-1 does not affect blood pressure or heart rate

A_{2A}R agonists evoke cardiovascular effects (Hutchison et al., 1989; Kirkup et al., 1998; Nekooeian and Tabrizchi, 1996). We therefore tested the effect of intraperitoneal administration of A_{2A}R PAM-1 on blood pressure and heart rate in wild-type mice. First, we measured blood pressure in mice 30, 90, and 150 min after intraperitoneal injection of 75 mg·kg^{-1} A_{2A}R PAM-1 or 1 mg·kg^{-1} of the A_{2A}R agonist CGS 21680 using an electrosphygmomanometer (**Figure 5A)**. The dose of the A_{2A}R agonist CGS 21680 was selected based on previous studies in mice (Carvalho et al., 2017; Nakav et al., 2008; Ohta and Sitkovsky, 2001). Compared with saline treatment, the systolic, and diastolic blood pressures were significantly decreased for up to 90 min after injecting the A_{2A}R agonist CGS 21680 (SBP at 30 min: $t_{(9)}$=10.55, P<0.0001, SBP at 90 min: $t_{(9)}$=7.51, P<0.0001, DBP at 30 min: $t_{(9)}$=6.60, P<0.0001, DBP at 90 min: $t_{(9)}$=5.86, P<0.0001, unpaired t-test) and returned to normal levels within 150 min after the injection. In contrast, blood pressure was not changed after intraperitoneal administration of A_{2A}R PAM-1 (75 mg·kg^{-1}) at 30, 90, or 150 min after treatment. In addition, we measured

455 the heart rate of mice after intraperitoneal injection of 75 mg·kg^{-1} A_{2A}R PAM-1 or 1
456 mg·kg^{-1} A_{2A}R agonist CGS 21680 using the telemetry implants (**Figure 5B**). The heart
457 rate of the mice increased after intraperitoneal administration of the A_{2A}R agonist CGS
458 21680 (HR at 60 min: $t_{(8)}$=2.34, P=0.047, HR at 75 min: $t_{(8)}$=2.90, P=0.019, HR at 90
459 min: $t_{(8)}$=2.80, P=0.023, unpaired t-test), whereas the heart rate was not affected by
460 injection of 75 mg·kg^{-1} A_{2A}R PAM-1. Finally, we monitored the heart rhythm in
461 anesthetized mice after intraperitoneal administration of 75 mg·kg^{-1} of A_{2A}R PAM-1 or
462 1 mg·kg^{-1} of A_{2A}R agonist CGS 21680 using intracardiac EGM. We observed sinus
463 arrhythmia in mice after intraperitoneal administration of A_{2A}R agonist CGS 21680,
464 whereas injection of 75 mg·kg^{-1} A_{2A}R PAM-1 did not cause abnormalities of the cardiac
465 rhythm (**Figure 5C**).
466
467 **4. Discussion**
468 Our observations suggest that enhancing A_{2A}R signaling by intraperitoneal
469 administration of A_{2A}R PAM-1 induces SWS without cardiovascular effects in mice.
470 Therefore, A_{2A}R-modulating compounds may provide safe options for the treatment of
471 insomnia and poor-quality sleep.
472 Over the past century, several putative hypnogenic substances implicated in the sleep
473 homeostatic process have been identified, including prostaglandin D_2 (Qu et al., 2006),
474 cytokines (Krueger et al., 1984), anandamide (García-García et al., 2009), urotensin II
475 peptide (Huitron-Resendiz et al., 2005), and adenosine (Porkka-Heiskanen et al., 1997).
476 Adenosine represents a state of relative energy deficiency: ATP depletion positively
477 correlates with an increase in extracellular adenosine levels (Kalinchuk et al., 2003)
478 and positively associates with sleep (Porkka-Heiskanen et al., 1997). Adenosine levels
479 in samples collected from several brain areas of cats during spontaneous sleep-wake

480 cycles by *in vivo* microdialysis were higher during SWS than during wakefulness for
481 all probed brain areas (Porkka-Heiskanen et al., 1997). The observation in animals that
482 adenosine levels are elevated during prolonged wakefulness may explain why an
483 allosteric modulator could effectively enhance the sleep-inducing effect of endogenous
484 adenosine in the brain. On the other hand, adenosine is absent or its concentration is
485 too low in the cardiovascular system under physiologic conditions to affect blood
486 pressure and heart function after administration of an allosteric modulator of $A_{2A}R$.
487 Medicinal chemistry for $A_{2A}Rs$ has been widely developed in recent decades for use in
488 myocardial perfusion imaging and the treatment of inflammation and neuropathic pain
489 (de Lera Ruiz et al., 2014). Several $A_{2A}R$ agonists that entered clinical trials elicited
490 undesirable side effects, however, thus precluding their further development. On the
491 other hand, allosteric modulators bind at a distinct site other than the natural ligand
492 binding site (i.e., the orthosteric site) and exert their effects only in the presence of the
493 orthosteric ligand (Wenthur et al., 2014). As a consequence, an allosteric modulator
494 mimics the activity duration of the natural ligand and thus the pharmacologic response
495 of an allosteric modulator more closely resembles the natural physiologic activity of
496 the receptor than is possible with a synthetic agonist. Because efforts to evoke
497 pharmacologic $A_{2A}R$ responses have focused almost exclusively on the use of
498 orthosteric ligands, however, the possibility that $A_{2A}R$ responses, especially in the brain,
499 can be fine-tuned using allosteric modulators has received very little attention (Göblyös
500 and Ijzerman, 2009).
501 Moreover, it is widely accepted that the basic adenosine scaffold must be maintained
502 in an $A_{2A}R$ agonist (Fredholm et al., 2011). Thus, the development of adenosine analogs
503 for treating the central nervous system, including sleep induction for treating insomnia,
504 is restricted by the poor transport of these drugs through the brain endothelial cells,

505 which are connected by tight junctions to establish a blood-brain barrier (BBB)
506 (Pardridge et al., 1994). In contrast, A_{2A}R PAM-1, when administered intraperitoneally,
507 exhibits a sleep-inducing effect that is likely mediated by A_{2A}Rs in the brain and thus
508 appears to cross the BBB. Small lipophilic monocarboxylates like A_{2A}R PAM-1 likely
509 pass through the BBB by passive diffusion or via a monocarboxylate transport system
510 (Tsuji, 2005). Therefore, allosteric modulation of A_{2A}Rs has the potential to cause
511 pharmacologic effects in the central nervous system after systemic administration,
512 resulting in good quality sleep.
513 Our study did not investigate how and where the A_{2A}R PAM-1 binds at the receptor to
514 exert its allosteric effect. Therefore, an important next step will be to examine the
515 allosteric interactions of A_{2A}R PAM-1 and the receptor using binding assays and crystal
516 structure analysis. With respect to the latter, a crystal structure of the human A_{2A}R
517 bound to a bitopic antagonist revealed a potential allosteric pocket (Sun et al., 2017)
518 and another study suggested that a sodium ion binding site can be exploited for
519 allosteric modulation of A_{2A}R (Gutiérrez-de-Terán et al., 2013). Moreover, to solidify
520 the sleep enhancing effect of the A_{2A}R PAM-1, it may be necessary to test the A_{2A}R
521 PAM-1 in mice at the time of normal sleep onset, i.e., A_{2A}R PAM-1 administration at
522 the onset of the light period, or in an animal model of insomnia, for example, a mouse
523 model mimicking the human first-night effect (Xu et al., 2014).
524 Due to work schedules and expectations, lifestyle choices, pre-existing medical
525 conditions, or aging, people are coping with an increasingly wide range of sleep
526 problems, including difficulties with falling and staying asleep, waking up too early,
527 and poor-quality ("non-restorative") sleep. Deficiencies in sleep cause significant social
528 losses due to increased prevalence of mood disorders, lead to decreased economic
529 productivity, and are linked to traffic and work-related accidents due to excessive

daytime sleepiness (Groeger et al., 2004; Saddichha, 2010; Sutton et al., 2001). Insufficient sleep is not only by itself a major problem in modern society, but is also an established risk factor for obesity, diabetes, heart disease, and other lifestyle diseases (Colten et al., 2006). Moreover, psychiatric illnesses, especially anxiety and mood disorders, are long recognized to be a frequent cause of insomnia (Okuji et al., 2002).

5. Conclusions

The findings of our study indicate that enhancing $A_{2A}R$ signaling promotes SWS without cardiovascular effects. Therefore, small molecules that allosterically modulate $A_{2A}Rs$ could help people with sleep problems to fall asleep and thus also be a potential treatment for psychiatric disorders.

Our study was conducted in mice, the most commonly used model organism of human disease. Results in mice, however, are not particularly reliable for predicting human study outcomes, mostly due to the limited genetic diversity associated with common laboratory mice. Therefore, many obstacles remain to be overcome in generating a novel drug for the treatment of insomnia in humans.

Conflicts of Interests

The authors declare no competing financial interests.

Author contributions

M.K., N.M., Y.C., F.S., and M.L. designed the experiments. M.K., F.D., R.Q., S.F., and X.Z. collected and analyzed the data. T.S., S.I., and H.N. synthesized chemical

compounds, J.C. and H.K. contributed mouse or cell lines, M.K., Y.C., and M.L. wrote the paper. All authors approved the final version of the manuscript.

Funding

This work was supported by the Japan Society for the Promotion of Science [Grant-in-Aid for Scientific Research B (grant number 17H02215) to M.L.]; the Japan Science and Technology Agency [CREST grant (grant number JPMJCR1655) to M.L.]; the Ministry of Education, Culture, Sports, Science, and Technology (MEXT) of Japan [Grants-in-Aid for Scientific Research on Innovative Areas "Living in Space" (grant numbers 15H05935, 15K21745, 18H04966) and "WillDynamics" (grant number 17H06047) to M.L.]; the World Premier International Research Center Initiative (WPI) from MEXT (to Y.C., T.S., H.N., and M.L.); and the Naito Foundation (to M.L.).

References

Aragona, M., 2000. Abuse, dependence, and epileptic seizures after zolpidem withdrawal: review and case report. Clin. Neuropharmacol. 23, 281–283.

Cai, X., Qian, C., Gould, S., Zhai, H., 2008. Multi-functional small molecules as anti-proliferative agents. US Patent 20080221132A1.

Carvalho, V.F., Ferreira, T.P.T., de Arantes, A.C.S., Noël, F., Tesch, R., Sant'Anna, C.M.R., Barreiro, E.J.L., Fraga, C.A.M., Rodrigues e Silva, P.M., Martins, M.A., 2017. LASSBio-897 Reduces Lung Injury Induced by Silica Particles in Mice: Potential Interaction with the A_2A Receptor. Front. Pharmacol. 8. https://doi.org/10.3389/fphar.2017.00778

Chen, J.F., Huang, Z., Ma, J., Zhu, J., Moratalla, R., Standaert, D., Moskowitz, M.A., Fink, J.S., Schwarzschild, M.A., 1999. A(2A) adenosine receptor deficiency

attenuates brain injury induced by transient focal ischemia in mice. J. Neurosci. 19, 9192–9200.

Chrivia, J.C., Kwok, R.P., Lamb, N., Hagiwara, M., Montminy, M.R., Goodman, R.H., 1993. Phosphorylated CREB binds specifically to the nuclear protein CBP. Nature 365, 855–859. https://doi.org/10.1038/365855a0

Colten HR, Altevogt BM, editors, Institute of Medicine (US) Committee on Sleep Medicine and Research, 2006. Sleep Disorders and Sleep Deprivation: An Unmet Public Health Problem. 3, Extent and Health Consequences of Chronic Sleep Loss and Sleep Disorders. National Academies Press, Washington, DC. Available from: https://www.ncbi.nlm.nih.gov/books/NBK19961/

Cox, C.D., Breslin, M.J., Whitman, D.B., Schreier, J.D., McGaughey, G.B., Bogusky, M.J., Roecker, A.J., Mercer, S.P., Bednar, R.A., Lemaire, W., Bruno, J.G., Reiss, D.R., Harrell, C.M., Murphy, K.L., Garson, S.L., Doran, S.M., Prueksaritanont, T., Anderson, W.B., Tang, C., Roller, S., Cabalu, T.D., Cui, D., Hartman, G.D., Young, S.D., Koblan, K.S., Winrow, C.J., Renger, J.J., Coleman, P.J., 2010. Discovery of the Dual Orexin Receptor Antagonist [(7R)-4-(5-Chloro-1,3-benzoxazol-2-yl)-7-methyl-1,4-diazepan-1-yl][5-methyl-2-(2H-1,2,3-triazol-2-yl)phenyl]methanone (MK-4305) for the Treatment of Insomnia. J. Med. Chem. 53, 5320–5332. https://doi.org/10.1021/jm100541c

de Lera Ruiz, M., Lim, Y.-H., Zheng, J., 2014. Adenosine A2A receptor as a drug discovery target. J. Med. Chem. 57, 3623–3650. https://doi.org/10.1021/jm4011669

de Zambotti, M., Goldstone, A., Colrain, I.M., Baker, F.C., 2017. Insomnia disorder in adolescence: Diagnosis, impact, and treatment. Sleep Med. Rev. https://doi.org/10.1016/j.smrv.2017.06.009

604 El Yacoubi, M., Ledent, C., Parmentier, M., Costentin, J., Vaugeois, J., 2000. SCH
605 58261 and ZM 241385 differentially prevent the motor effects of CGS 21680 in
606 mice: evidence for a functional “atypical” adenosine A(2A) receptor. Eur. J.
607 Pharmacol. 401, 63–77.
608 Fredholm, B.B., IJzerman, A.P., Jacobson, K.A., Linden, J., Müller, C.E., 2011.
609 International Union of Basic and Clinical Pharmacology. LXXXI. Nomenclature
610 and classification of adenosine receptors--an update. Pharmacol. Rev. 63, 1–34.
611 https://doi.org/10.1124/pr.110.003285
612 García-García, F., Acosta-Peña, E., Venebra-Muñoz, A., Murillo-Rodríguez, E., 2009.
613 Sleep-inducing factors. CNS Neurol. Disord. Drug Targets 8, 235–244.
614 Göblyös, A., Ijzerman, A.P., 2009. Allosteric modulation of adenosine receptors.
615 Purinergic Signal. 5, 51–61. https://doi.org/10.1007/s11302-008-9105-3
616 Groeger, J.A., Zijlstra, F.R.H., Dijk, D.-J., 2004. Sleep quantity, sleep difficulties and
617 their perceived consequences in a representative sample of some 2000 British
618 adults. J. Sleep Res. 13, 359–371. https://doi.org/10.1111/j.1365-
619 2869.2004.00418.x
620 Gutiérrez-de-Terán, H., Massink, A., Rodríguez, D., Liu, W., Han, G.W., Joseph, J.S.,
621 Katritch, I., Heitman, L.H., Xia, L., IJzerman, A.P., Cherezov, V., Katritch, V.,
622 Stevens, R.C., 2013. The Role of a Sodium Ion Binding Site in the Allosteric
623 Modulation of the A_{2A} Adenosine G Protein-Coupled Receptor. Structure 21,
624 2175–2185. https://doi.org/10.1016/j.str.2013.09.020
625 Huitron-Resendiz, S., Kristensen, M.P., Sánchez-Alavez, M., Clark, S.D., Grupke,
626 S.L., Tyler, C., Suzuki, C., Nothacker, H.-P., Civelli, O., Criado, J.R., Henriksen,
627 S.J., Leonard, C.S., de Lecea, L., 2005. Urotensin II modulates rapid eye

movement sleep through activation of brainstem cholinergic neurons. J. Neurosci. 25, 5465–5474. https://doi.org/10.1523/JNEUROSCI.4501-04.2005

Hutchison, A.J., Webb, R.L., Oei, H.H., Ghai, G.R., Zimmerman, M.B., Williams, M., 1989. CGS 21680C, an A_2 selective adenosine receptor agonist with preferential hypotensive activity. J. Pharmacol. Exp. Ther. 251, 47–55.

Jacobson, L.H., Callander, G.E., Hoyer, D., 2014. Suvorexant for the treatment of insomnia. Expert Rev. Clin. Pharmacol. 7, 711–730. https://doi.org/10.1586/17512433.2014.966813

Kalinchuk, A.V., Urrila, A.-S., Alanko, L., Heiskanen, S., Wigren, H.-K., Suomela, M., Stenberg, D., Porkka-Heiskanen, T., 2003. Local energy depletion in the basal forebrain increases sleep. Eur. J. Neurosci. 17, 863–869.

Kirkup, A.J., Eastwood, C., Grundy, D., Chessell, I.P., Humphrey, P.P., 1998. Characterization of adenosine receptors evoking excitation of mesenteric afferents in the rat. Br. J. Pharmacol. 125, 1352–1360. https://doi.org/10.1038/sj.bjp.0702202

Kitamura, T., Koshino, Y., Shibata, F., Oki, T., Nakajima, H., Nosaka, T., Kumagai, H., 2003. Retrovirus-mediated gene transfer and expression cloning: powerful tools in functional genomics. Exp. Hematol. 31, 1007–1014. https://doi.org/10.1016/j.exphem.2003.07.005

Krueger, J.M., Walter, J., Dinarello, C.A., Wolff, S.M., Chedid, L., 1984. Sleep-promoting effects of endogenous pyrogen (interleukin-1). Am. J. Physiol. 246, R994-999.

Methippara, M.M., Kumar, S., Alam, M.N., Szymusiak, R., McGinty, D., 2005. Effects on sleep of microdialysis of adenosine A_1 and A_{2a} receptor analogs into

652 the lateral preoptic area of rats. Am. J. Physiol. Regul. Integr. Comp. Physiol.
653 289, R1715-1723. https://doi.org/10.1152/ajpregu.00247.2005
654
655 Montminy, M.R., Gonzalez, G.A., Yamamoto, K.K., 1990. Regulation of cAMP-
656 inducible genes by CREB. Trends Neurosci. 13, 184–188.
657 Morita, S., Kojima, T., Kitamura, T., 2000. Plat-E: an efficient and stable system for
658 transient packaging of retroviruses. Gene Ther. 7, 1063–1066.
659 https://doi.org/10.1038/sj.gt.3301206
660 Nakamura, Y., Midorikawa, T., Monoi, N., Kimura, E., Murata-Matsuno, A., Sano,
661 T., Oka, K., Sugafuji, T., Uchiyama, A., Murakoshi, M., Sugiyama, K., Nishino,
662 H., Urade, Y., 2016. Oral administration of Japanese sake yeast (Saccharomyces
663 cerevisiae sake) promotes non-rapid eye movement sleep in mice via adenosine
664 A_{2A} receptors. J. Sleep Res. 25, 746–753. https://doi.org/10.1111/jsr.12434
665 Nakav, S., Chaimovitz, C., Sufaro, Y., Lewis, E.C., Shaked, G., Czeiger, D., Zlotnik,
666 M., Douvdevani, A., 2008. Anti-Inflammatory Preconditioning by Agonists of
667 Adenosine A_1 Receptor. PLoS ONE 3.
668 https://doi.org/10.1371/journal.pone.0002107
669 National Research Council, 2011. Guide for the care and use of laboratory animals.
670 8th ed. National Academy Press, Washington, DC.
671 Nekooeian, A.A., Tabrizchi, R., 1996. Effects of adenosine A2A receptor agonist,
672 CGS 21680, on blood pressure, cardiac index and arterial conductance in
673 anaesthetized rats. Eur. J. Pharmacol. 307, 163–169.
674 Ohta, A., Sitkovsky, M., 2001. Role of G-protein-coupled adenosine receptors in
675 downregulation of inflammation and protection from tissue damage. Nature 414,
676 916–920. https://doi.org/10.1038/414916a

677 Oishi, Y., Takata, Y., Taguchi, Y., Kohtoh, S., Urade, Y., Lazarus, M., 2016.
678 Polygraphic Recording Procedure for Measuring Sleep in Mice. J. Vis. Exp.
679 e53678–e53678. https://doi.org/10.3791/53678
680 Okuji, Y., Matsuura, M., Kawasaki, N., Kometani, S., Shimoyama, T., Sato, M., Oga,
681 K., Abe, K., 2002. Prevalence of insomnia in various psychiatric diagnostic
682 categories. Psychiatry Clin. Neurosci. 56, 239–240.
683 https://doi.org/10.1046/j.1440-1819.2002.01012.x
684 Pardridge, W.M., Yoshikawa, T., Kang, Y.S., Miller, L.P., 1994. Blood-brain barrier
685 transport and brain metabolism of adenosine and adenosine analogs. J.
686 Pharmacol. Exp. Ther. 268, 14–18.
687 Paxinos, G., Franklin, K.B.J., 2004. The Mouse Brain in Stereotaxic Coordinates.
688 Second ed. Academic Press, Cambridge, MA.
689 Porkka-Heiskanen, T., Strecker, R.E., Thakkar, M., Bjorkum, A.A., Greene, R.W.,
690 McCarley, R.W., 1997. Adenosine: a mediator of the sleep-inducing effects of
691 prolonged wakefulness. Science 276, 1265–1268.
692 Qu, W.-M., Huang, Z.-L., Xu, X.-H., Aritake, K., Eguchi, N., Nambu, F., Narumiya,
693 S., Urade, Y., Hayaishi, O., 2006. Lipocalin-type prostaglandin D synthase
694 produces prostaglandin D_2 involved in regulation of physiological sleep. Proc.
695 Natl. Acad. Sci. U.S.A. 103, 17949–17954.
696 https://doi.org/10.1073/pnas.0608581103
697 Roth, T., 2007. Insomnia: Definition, Prevalence, Etiology, and Consequences. J.
698 Clin. Sleep Med. 3, S7–S10.
699 Saddichha, S., 2010. Diagnosis and treatment of chronic insomnia. Ann. Indian Acad.
700 Neurol. 13, 94–102. https://doi.org/10.4103/0972-2327.64628

Satoh, S., Matsumura, H., Koike, N., Tokunaga, Y., Maeda, T., Hayaishi, O., 1999. Region-dependent difference in the sleep-promoting potency of an adenosine A_{2A} receptor agonist. Eur. J. Neurosci. 11, 1587–1597.

Scammell, T.E., Gerashchenko, D.Y., Mochizuki, T., McCarthy, M.T., Estabrooke, I.V., Sears, C.A., Saper, C.B., Urade, Y., Hayaishi, O., 2001. An adenosine A_{2A} agonist increases sleep and induces Fos in ventrolateral preoptic neurons. Neuroscience 107, 653–663.

Seow, L.S.E., Abdin, E., Chang, S., Chong, S.A., Subramaniam, M., 2018. Identifying the best sleep measure to screen clinical insomnia in a psychiatric population. Sleep Med. 41, 86–93. https://doi.org/10.1016/j.sleep.2017.09.015

Sun, B., Bachhawat, P., Chu, M.L.-H., Wood, M., Ceska, T., Sands, Z.A., Mercier, J., Lebon, F., Kobilka, T.S., Kobilka, B.K., 2017. Crystal structure of the adenosine A_{2A} receptor bound to an antagonist reveals a potential allosteric pocket. Proc. Natl. Acad. Sci. U. S. A. 114, 2066–2071. https://doi.org/10.1073/pnas.1621423114

Sutton, D.A., Moldofsky, H., Badley, E.M., 2001. Insomnia and health problems in Canadians. Sleep 24, 665–670.

Tsuji, A., 2005. Small molecular drug transfer across the blood-brain barrier via carrier-mediated transport systems. NeuroRx 2, 54–62. https://doi.org/10.1602/neurorx.2.1.54

Urade, Y., Eguchi, N., Qu, W.-M., Sakata, M., Huang, Z.-L., Chen, J.-F., Schwarzschild, M.A., Fink, J.S., Hayaishi, O., 2003. Sleep regulation in adenosine A_{2A} receptor-deficient mice. Neurology 61, S94-96.

Vgontzas, A.N., Kales, A., Bixler, E.O., 1995. Benzodiazepine side effects: role of pharmacokinetics and pharmacodynamics. Pharmacology 51, 205–223.

726 Wafford, K.A., Ebert, B., 2008. Emerging anti-insomnia drugs: tackling sleeplessness
727 and the quality of wake time. Nat. Rev. Drug Discov. 7, 530–540.
728 https://doi.org/10.1038/nrd2464
729 Wenthur, C.J., Gentry, P.R., Mathews, T.P., Lindsley, C.W., 2014. Drugs for
730 allosteric sites on receptors. Annu. Rev. Pharmacol. Toxicol. 54, 165–184.
731 https://doi.org/10.1146/annurev-pharmtox-010611-134525
732 Xu, Q., Xu, X.-H., Qu, W.-M., Lazarus, M., Urade, Y., Huang, Z.-L., 2014. A mouse
733 model mimicking human first night effect for the evaluation of hypnotics.
734 Pharmacol. Biochem. Behav. 116, 129–136.
735 https://doi.org/10.1016/j.pbb.2013.11.029

Figures and legends

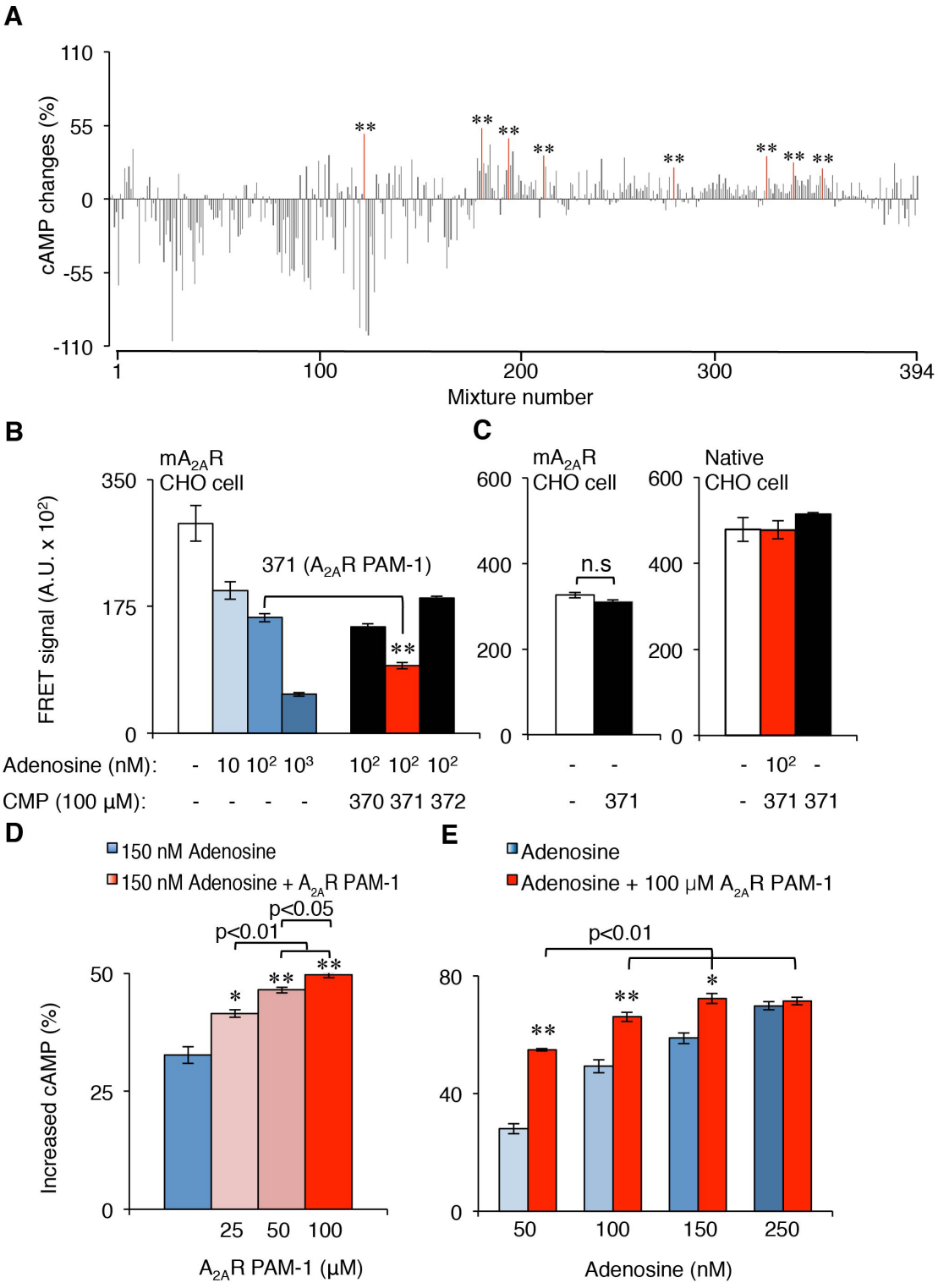

Fig. 1. Co-treatment of mA$_{2A}$R-CHO cells with A$_{2A}$R PAM-1 and adenosine revealed allosteric modulation. (A) High-throughput screening of small-molecule compounds. Changes of cAMP levels in CHO cells after treatment with adenosine and compound

741 mixtures are shown as percentage of cAMP levels in CHO cells after treatment with
742 adenosine. Screening experiments were performed in triplicate wells. (B) FRET
743 activity in $mA_{2A}R$-expressing CHO cells after treatment with adenosine and small
744 molecule compounds 370, 371, or 372. (C) FRET activity in $mA_{2A}R$-expressing (left
745 panel) and native (right panel) CHO cells after treatment with adenosine or adenosine
746 and $A_{2A}R$ PAM-1, respectively. (D, E) Dose-dependent changes of cAMP level in
747 $mA_{2A}R$-expressing CHO cells after treatment with adenosine and different
748 concentrations of $A_{2A}R$ PAM-1 (D) or $A_{2A}R$ PAM-1 and different concentrations of
749 adenosine (E). (B-E) Experiments were performed in triplicate wells for each condition
750 and repeated at least twice. Representative data are shown. Data are presented as mean
751 ± SEM.

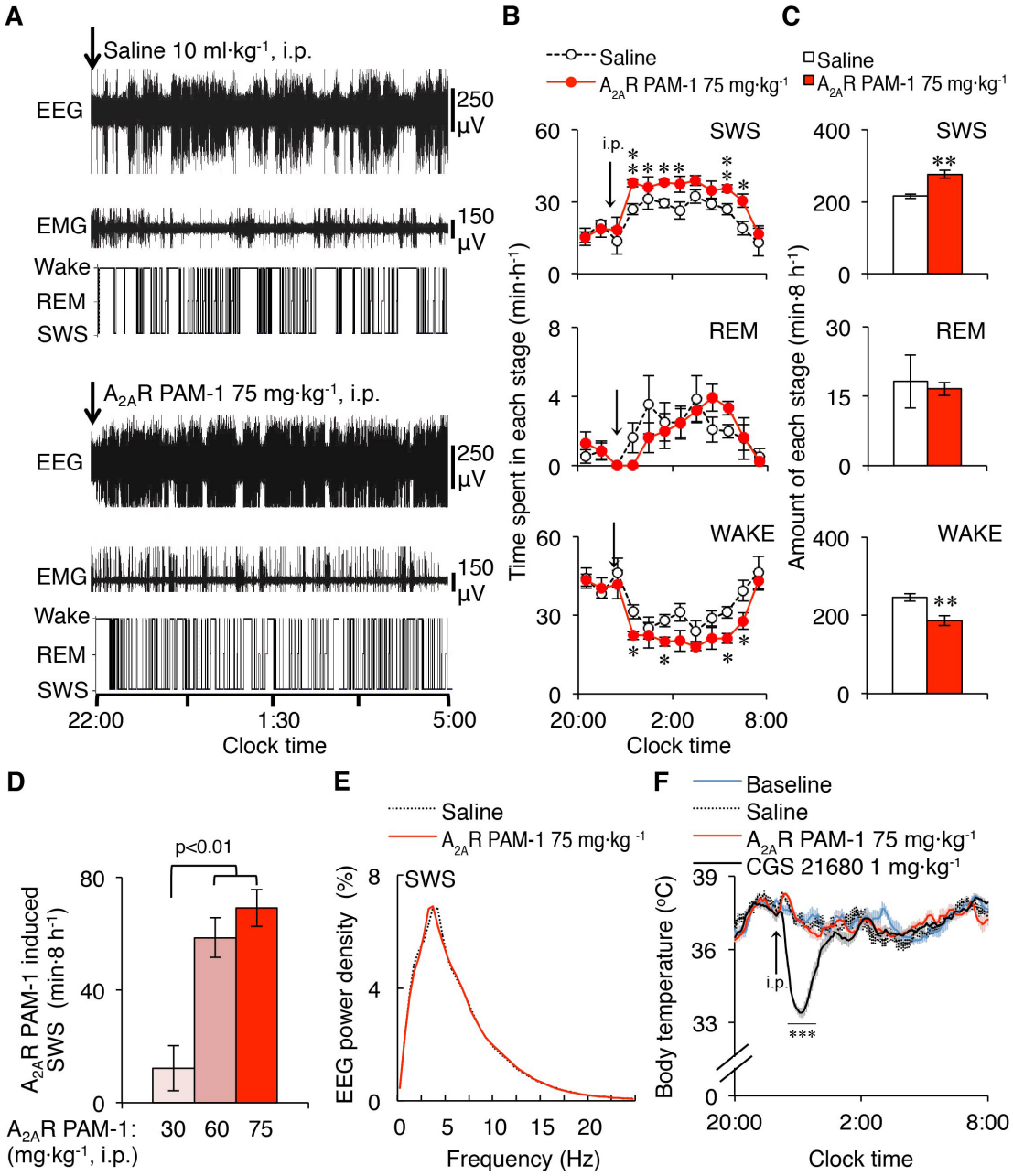

Fig. 2. Intraperitoneal administration of A_{2A}R PAM-1 induces SWS without affecting body temperature in mice. (A) Typical examples of EEG, EMG, and hypnograms of a mouse after the administration of saline (top panel) or A_{2A}R PAM-1 (bottom panel). (B, C) Time-courses (B) and total amounts (C) of SWS, REM sleep, and wakefulness in mice after intraperitoneal administration of saline or A_{2A}R PAM-1. (D) Dose-dependent changes in SWS time during 8 h after A_{2A}R PAM-1 administration normalised to the SWS time of the vehicle control. (E) EEG power density of SWS for

8 h after saline or $A_{2A}R$ PAM-1 administration. Data are presented as mean ± SEM (n=5/group). (F) Body temperature of mice after intraperitoneal administration of saline, $A_{2A}R$ PAM-1 or CGS 21680. Data are presented as mean ± SEM (n=6/group).

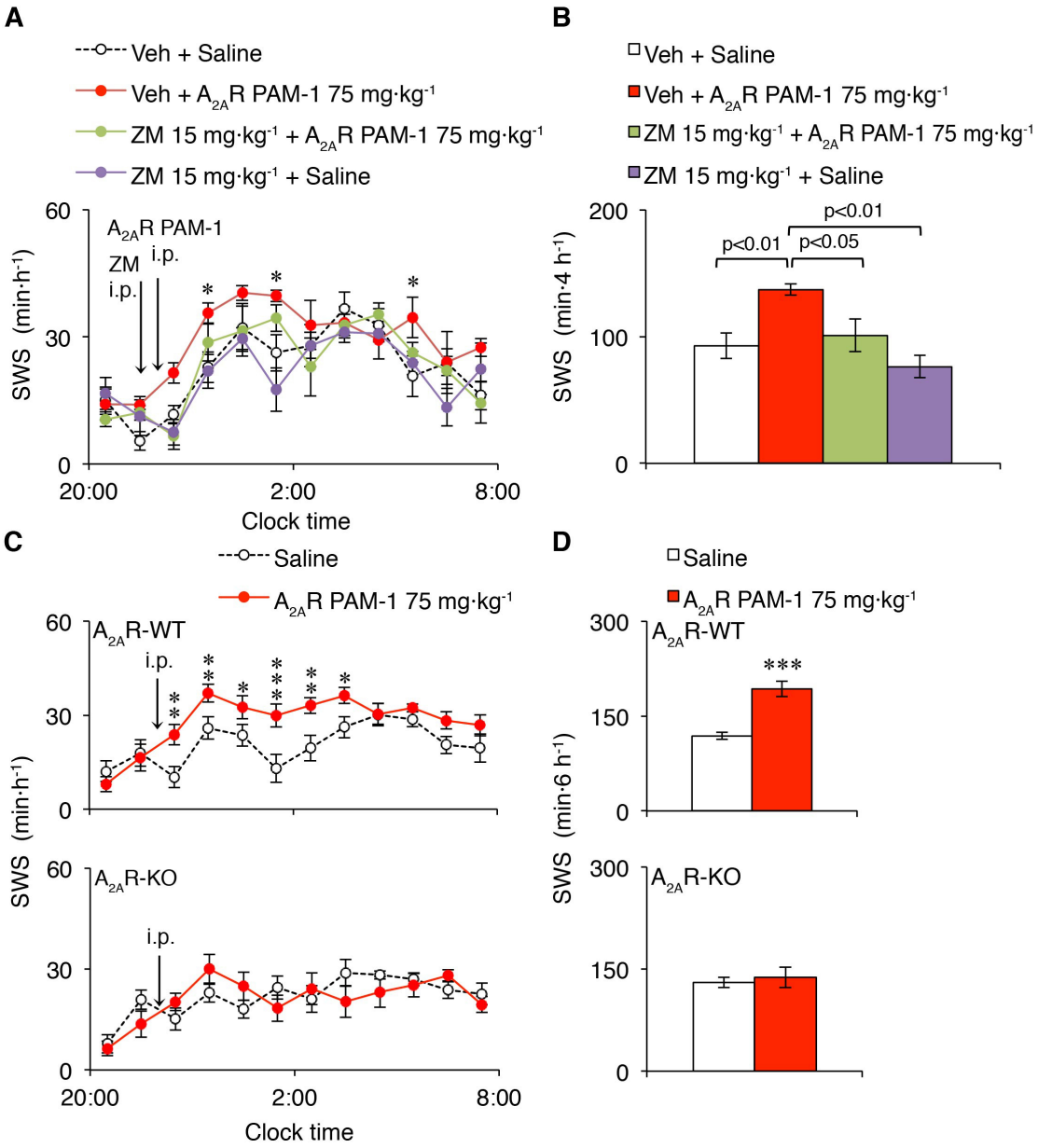

Fig. 3. Sleep inducing effect of $A_{2A}R$ PAM-1 depends on adenosine $A_{2A}R$ in mice. (A, B) Time-courses (A) and total amount (B) of SWS in mice pretreated with vehicle or the $A_{2A}R$ antagonist ZM 241385 after administration of saline or $A_{2A}R$ PAM-1 (n=5/group, respectively). (C, D) Time-courses (C) and total amount (D) of SWS in

wild-type (top panels) or $A_{2A}R$ KO mice (bottom panels) after administration of saline or $A_{2A}R$ PAM-1 (8/group). Data are presented as mean ± SEM.

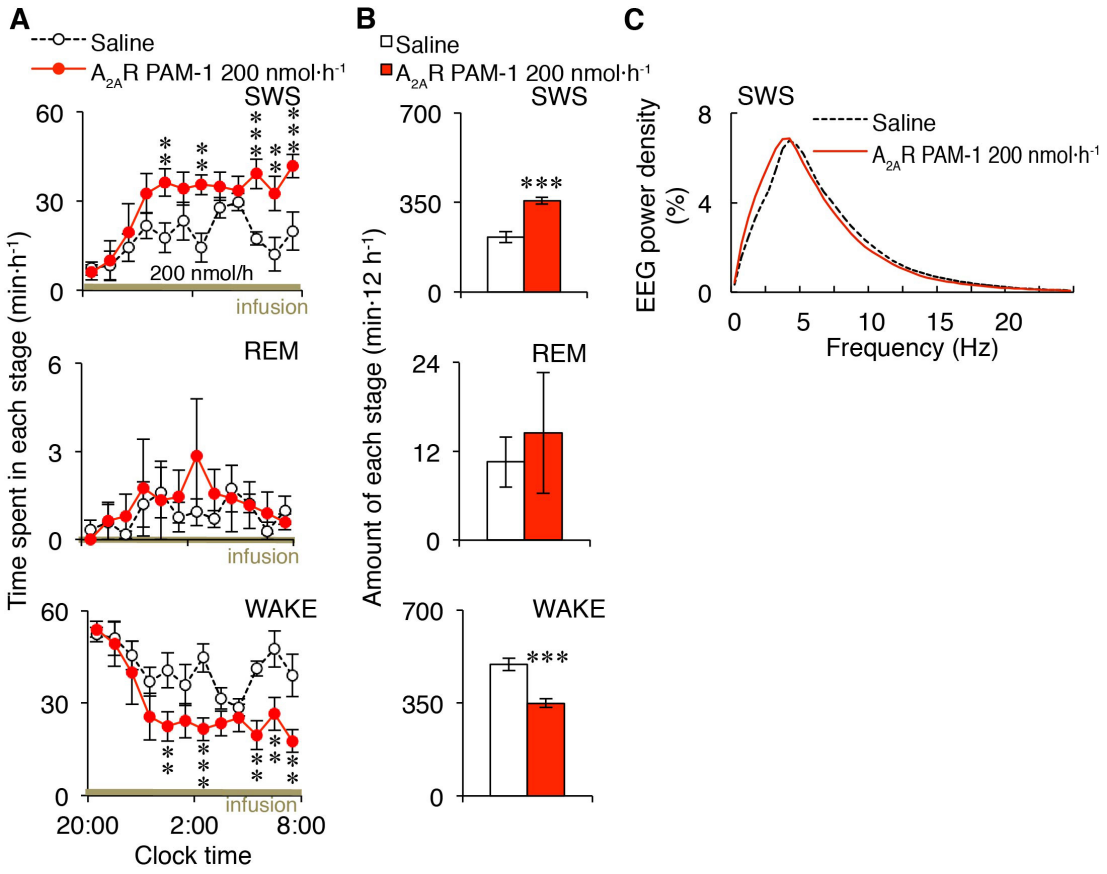

Fig. 4. Intracerebroventricular infusion of $A_{2A}R$ PAM-1 induced SWS in mice. (A, B) Time-courses (A) and total amount of SWS, REM sleep, and wakefulness (B) in mice after intracerebroventricular infusion of saline or $A_{2A}R$ PAM-1. (C) EEG power density of SWS during the infusion of saline or $A_{2A}R$ PAM-1. Data are presented as mean ± SEM (n=5/group).

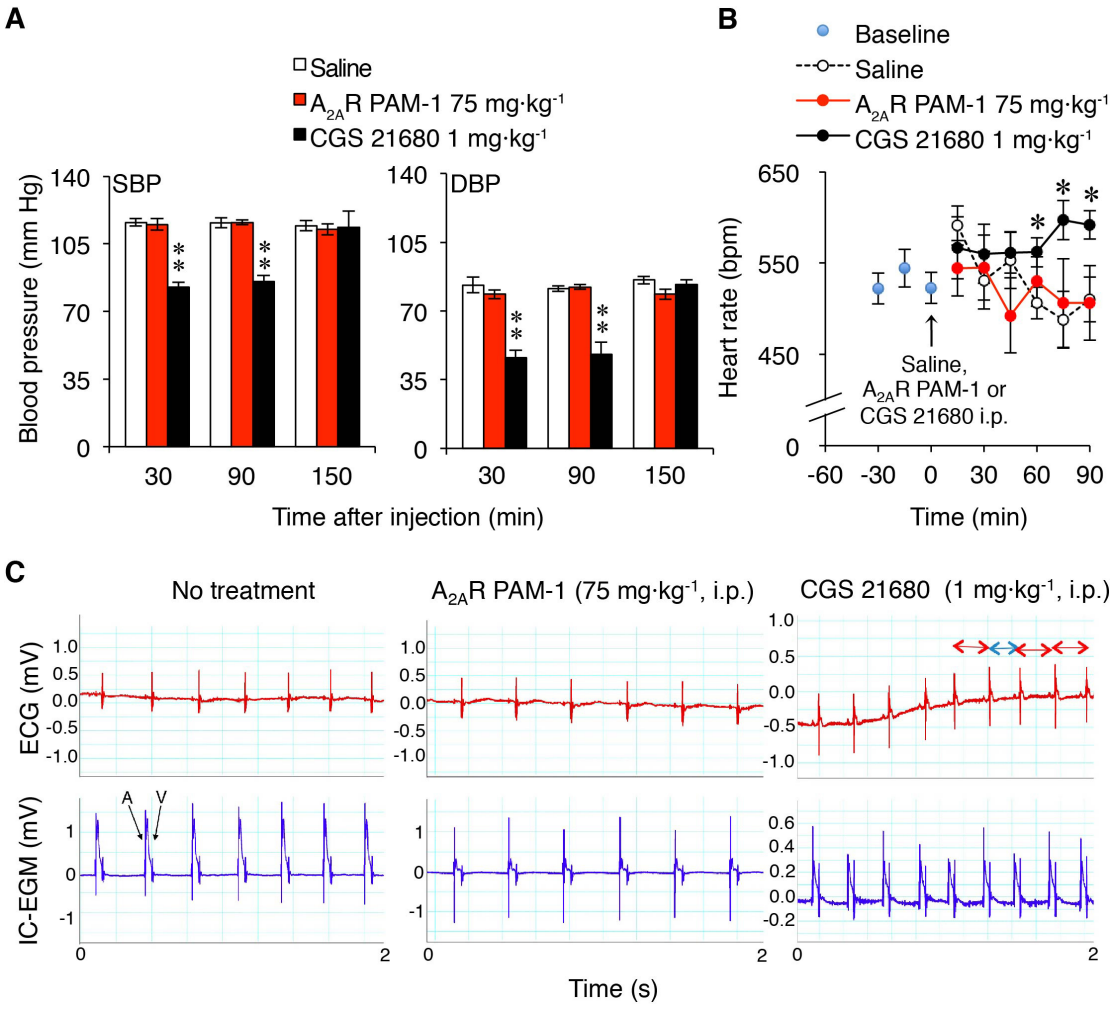

Fig. 5. $A_{2A}R$ PAM-1 does not affect the cardiovascular system. (A) Systolic, and diastolic blood pressure after $A_{2A}R$ PAM-1 or CGS 21680 injection in mice (n=5/group). (B) Heart rate of mice after injection of saline, $A_{2A}R$ PAM-1, or CGS 21680, assessed by the telemetry implants (n=5/group). (A, B) Data are presented as mean ± SEM. (C) Typical heart rhythm profiles of mice without treatment (left panel) or after administration of $A_{2A}R$ PAM-1 (middle panel) or CGS 21680 (right panel). Red and blue left/right arrows in the right panel indicate sinus arrhythmia. Abbreviations used: SBP, systolic blood pressure; DBP, diastolic blood pressure; ECG, electrocardiogram; IC-EGM, intracardiac electrogram; A, atrial signal; V, ventricular signal.

Supplementary figures and legends

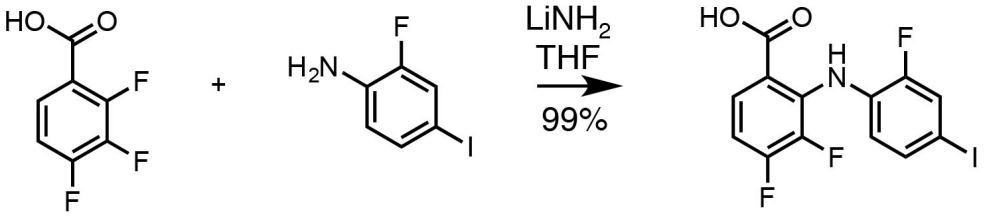

1 2 3

Fig. S1. Chemical synthesis of $A_{2A}R$ PAM-1. $A_{2A}R$ PAM-1 (3) was produced by combining 2,3,4-fluorobenzoic acid (1) and 2-fluoro-4-iodoaniline (2).

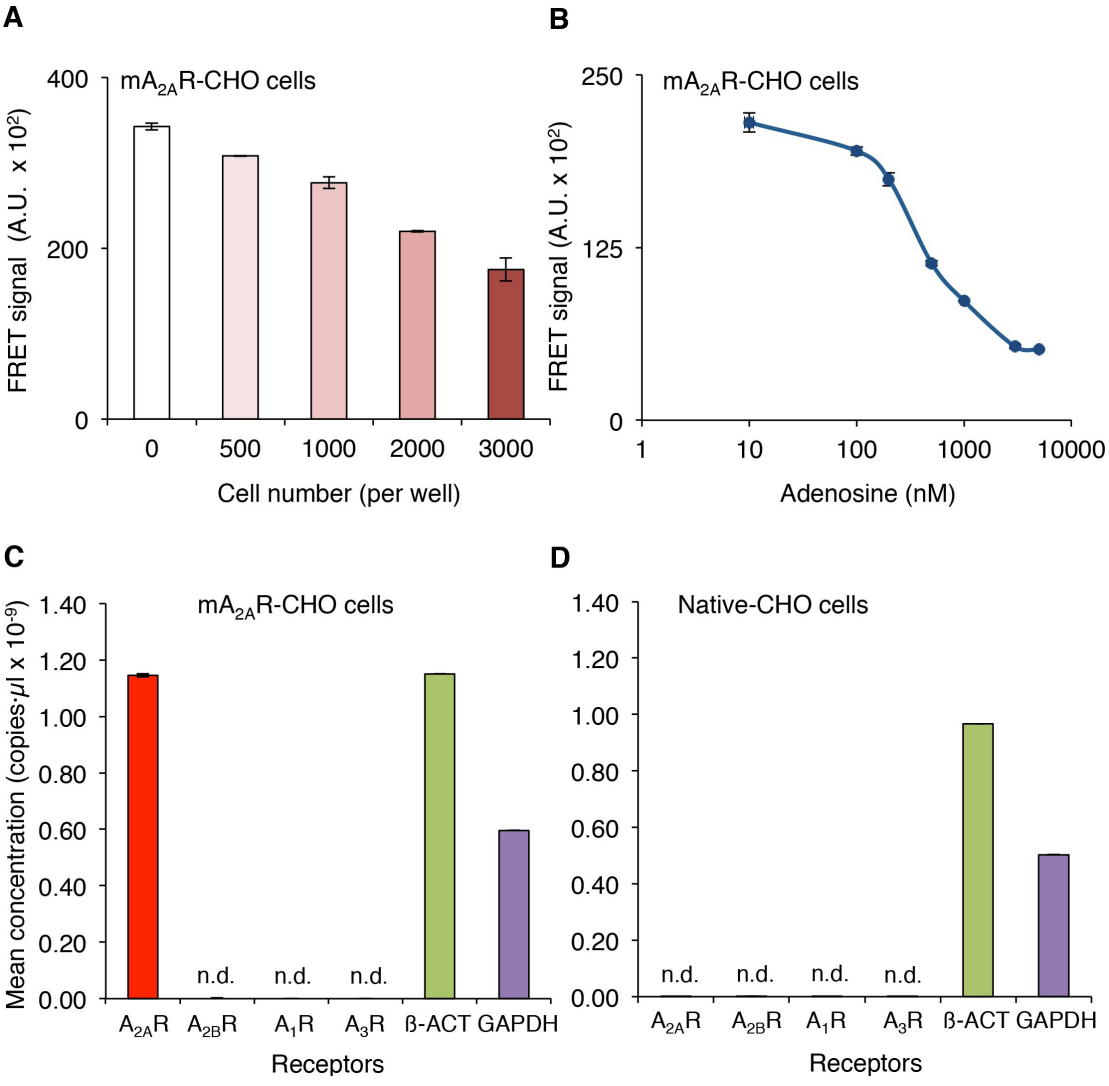

Fig. S2. Characterization of mouse $A_{2A}R$-expressing CHO cells. (A) Cell number-dependent FRET activity of $mA_{2A}R$-expressing CHO. (B) Dose-dependent changes of

FRET activity in mA$_{2A}$R-expressing CHO after adenosine administration. (C) Expression of Chinese hamster adenosine receptors in mA$_{2A}$R-expressing (left panel) and native (right panel) CHO cells.

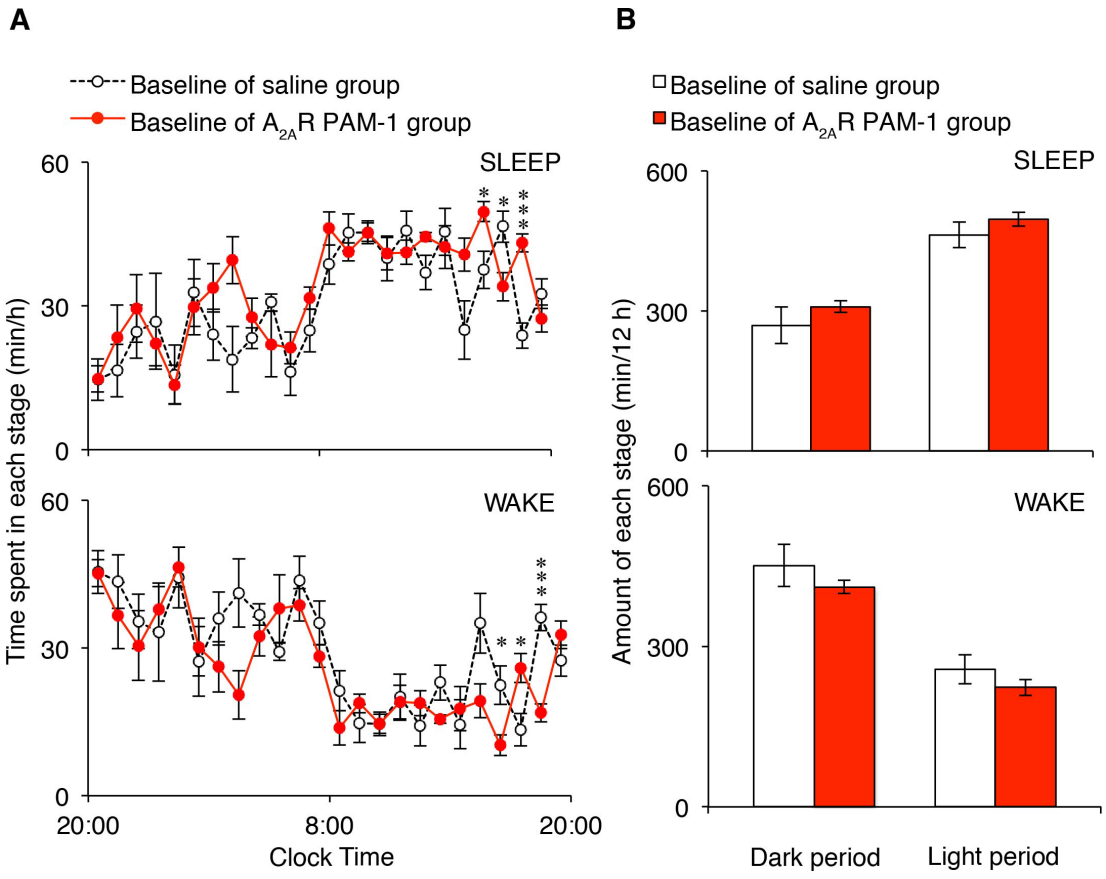

Fig. S3. Baseline sleep/wake profile of the mice before treatment. (A, B) Time-courses (A) and total amount of sleep (top panels; combined SWS and REM sleep amounts) and wakefulness (bottom panels) in mice over 24 h. Data are presented as mean ± SEM (n=5/group).

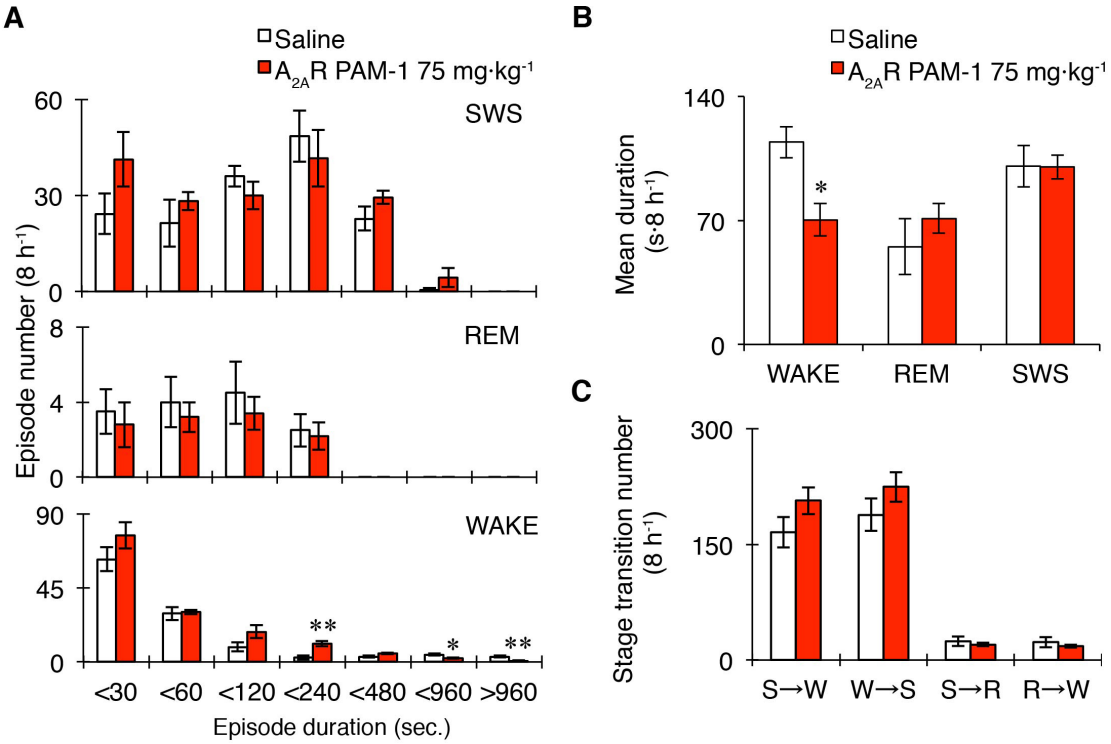

807

808 **Fig. S4.** Sleep architecture of mice after intraperitoneal administration of $A_{2A}R$ PAM-

809 1. (A, B) Episode number (A) and mean duration (B) of each stage after administration

810 of saline or $A_{2A}R$ PAM-1. (C) Transitions between SWS (S), REM sleep (R), and wake

811 (W) stages after administration of saline or $A_{2A}R$ PAM-1. Data are presented as mean

812 ± SEM (n=5/group).

813

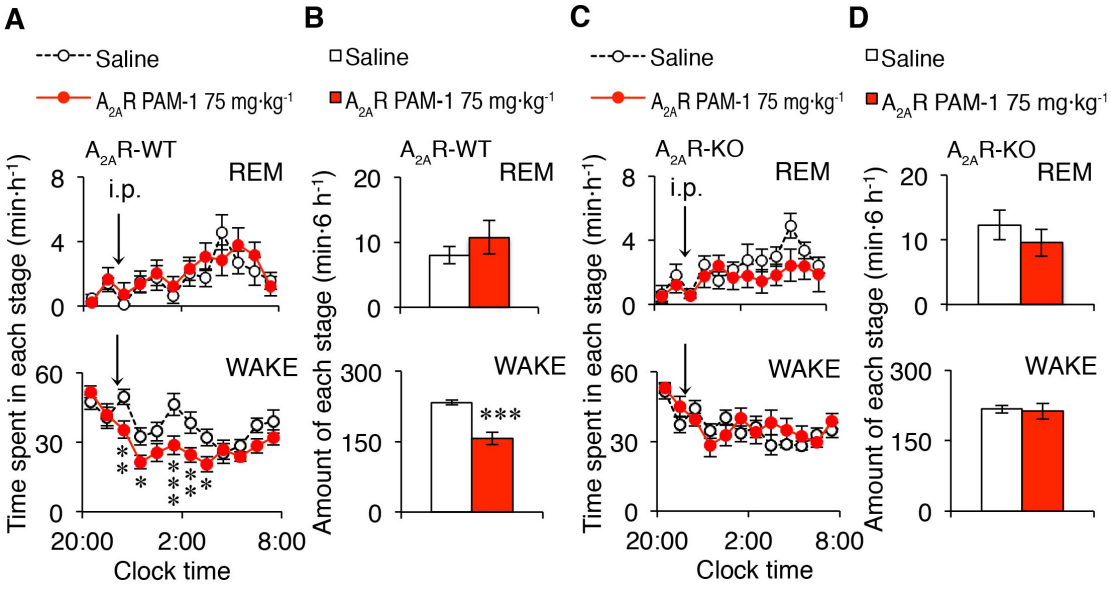

814

Fig. S5. REM sleep and wakefulness in wild-type and $A_{2A}R$ KO mice after intraperitoneal administration of $A_{2A}R$ PAM-1. (A-D) Time-courses (A and C) and total amount (B and D) of REM sleep (top panels) and wakefulness (bottom panels) in wild-type (A and B) and $A_{2A}R$ KO mice (C and D). Data are presented as mean ± SEM (n=8/group).

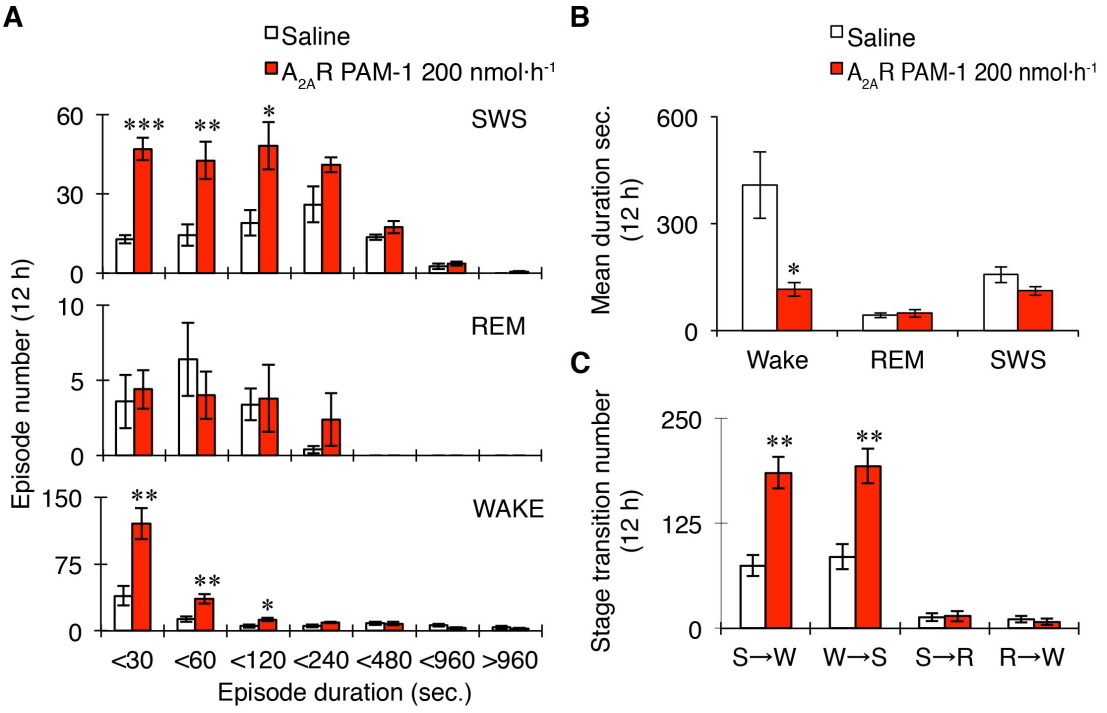

Fig. S6. Sleep architecture of mice after intracerebroventricular infusion of $A_{2A}R$ PAM-1. (A, B) Episode number (A) and mean duration (B) of each stage after infusion of saline or $A_{2A}R$ PAM-1. (C) Transitions between SWS (S), REM sleep (R), and wake (W) stages after infusion of saline or $A_{2A}R$ PAM-1. Data are presented as mean ± SEM (n=5/group).